Laves-phase evolution during aging in fine grained heat-affected zone of a tungsten-strengthened 9%Cr steel weldment

Xue Wang [a, *], Qiang Xu [b], Shu-min Yu [a], Hong Liu [c], Lei Hu [a], Yao-yao Ren [a]

[a] *School of Power and Mechanics, Wuhan University, Wuhan 430072, China*

[b] *School of Computing and Engineering, The University of Huddersfield, Huddersfield, HD1 3DH, England*

[c] *DongFang Boiler Group Co.,Ltd.，Zigong 643001, China*

Accepted version and its final version was published in *Journal of Materials Processing Technology*, 219. pp. 60-69. ISSN 0924-0136

Abstract— The precipitation and coarsening of Laves-phase in the fine grained heat-affected zone（FGHAZ） of a 9% Cr steel P92 welded joint during thermal aging at 923 K were investigated and compared to the base metal (BM), in order to clarify their effects on the Type Ⅳ fracture. Laves-phase precipitated mostly on the prior austenite grain boundaries of the FGHAZ. In comparison with BM, FGHAZ contained more grain boundary areas and can provide more nucleation sites for Laves-phase, resulting in an accelerated precipitation and rapidly reaching to the around 1.0% of saturated volume fraction. The coarsening of Laves-phase precipitates in FGHAZ was also much faster than that in BM, enhanced by the contribution of grain boundary diffusion resulted from its finer prior austenite grains. The FGHAZ had denser and smaller Laves-phase precipitates during the precipitation period in comparison with BM, obviously improved the creep strength by precipitation hardening. However, this effect in FGHAZ reduced sharply during coarsening owing to its coarsening rate greater than that of BM. In addition to the initial coarse polygonal subgrains with low dislocation density in FGHAZ produced by the weld thermal cycle and subsequent tempering in post-weld heat treatment（PWHT）, coarse Laves-phase precipitates on grain boundaries formed in the long-term thermal aging, contributing to the formation of the creep cavities, can also play a key role in Type Ⅳ fracture of welded joint in 9% Cr steels.

Keywords: Alloys; Welding; Precipitation and Coarsening; Electron Microscopy; Microstructure

Corresponding author. Tel.: +86 13554693820; fax: +86 02768772253.
E-mail address: wxue2011@whu.edu.cn (Xue Wang)

1. Introduction

High Cr martensitic heat resistant steels are key materials for the main steam pipe and header with larger

Corresponding author. Tel.: +86 13554693820; fax: +86 02768772253.
E-mail address: wxue2011@whu.edu.cn (Xue Wang)

diameter and thick wall in ultra-supercritical (USC) plant, because of their low thermal expansion coefficient, good corrosion resistance, good fabricability and especially their high creep rupture strength. Tshuchida et al.（1995） and Muramatasa（1998）regarded the ASME P92（9Cr-0.5Mo-1.8WVNb）strengthened by W as the most potential material for these applications. However, Matsui et al.（2001）and Wang et al.（2012） found that the application of such steels is hampered by the Type IV failure, where cracks occurred in the fine grained heat affected zone (FGHAZ) of weld. Accordingly, it is important to clarify the mechanisms of Type Ⅳ cracking and find out the factors affecting it. There have been a number of microstructure evolution investigations related to the creep property deterioration in FGHAZ. Letofsky and Cerjak（2004） investigated the metallography of the HAZ in tungsten alloyed 9% Cr steel weld and suggested that the reduction of the dislocation density and the recovery process（formation and growth of subgrain boundaries）are responsible for the drop of the creep resistance in the HAZ. Abe and Tabuchi（2004）described the undissolved $M_{23}C_6$ carbides of FGHAZ are coarsened during the post weld heat treatment（PWHT）, resulting in the degradation of creep rupture strength. Tsuchida et al.（1996）reported that HAZ softening of Mod.9Cr-1Mo steel is probably due to the lack of fine Nb and V precipitates coherent with the matrix, which is closely associated with little dissolution and coarsening of these precipitates by welding thermal cycle. Dejun et al.（2003）and El-Azim et al.（2005）revealed that the finer prior austenite grain size of the FGHAZ in high Cr steel welds is the most significant factor as it accelerates the rate of growth of martensite lath subgrains. The results of these investigations have shown that the microstructural changes in FGHAZ occurred during weld thermal cycle and subsequent post-weld heat treatment（PWHT）. As Type Ⅳ cracking takes place in long-term service under low stress conditions, studies on microstructural evolution during creep exposure, such as the formation of Laves-phase and Z-phase, are also required to better understand the factors affecting Type Ⅳ cracking. However, to date, the research on the precipitation behavior of the two secondary phases in FGHAZ was little.

Recently, Parker（2013） has reported the microstructure difference/ characteristic of HAZ and advocated the potential importance of cavity in determining the creep life/rupture. Xu et al.（2013） argued that creep damage of material was affected and controlled by the coupling of the microstructural instability (under thermal exposure and stress) and the cavitation. Furthermore, they summarized published literatures tentatively and specifically suggesting the link between laves-phase and cavitation which led to ultimate failure. Thus, Xu et al.（2013） pointed out that in order to provide a systematic and definite understanding of that process and the creep damage, it is necessary to sequentially investigate that 1) the Laves-phase precipitation and coarsening during the thermal exposure; 2) the Laves-phase precipitation and coarsening under creep (both uniaxial and multi-axial states of stress); 3) the cavitation under creep (both under uniaxial and multi-axial states of stress). This is true for base steel and weld.

Due to the small size of FGHAZ in an actual weld, simulation method has to be utilized. Wang et al.（2014） have investigated and reported the feasibility of such method.

Laves-phase is an intermetallic phase [（Fe,Cr）$_2$(Mo,W)] along grain boundaries and lath boundaries, which appears during thermal aging or creep but does not exist in tempering condition. Lee et al.（2006） and Wang et al.（2012） reported the precipitation of Laves-phase affected the degradation of creep rupture strength and fracture behavior of BM and welded joint, respectively. The precipitation and coarsening behavior of Laves-phase in FGHAZ may be markedly different from that in BM, produced by the considerable different size of prior austenite gain. Therefore, Laves-phase evolution in FGHAZ should be systematically investigated to clarify its effect on the Type Ⅳ cracking. In the present work, the quantification of Laves-phase was carried out on the FGHAZ specimens aged at 923 K for up to 5000 h. The results obtained from the FGHAZ were compared to that of BM to investigate their differences of Laves-phase reactions. Based on the analyses of precipitation and coarsening behavior of Laves-phase, its influence on the deterioration of creep rupture strength of FGHAZ was discussed.

Because the HAZ of real welded joints is limited to only a small volume, uniform microstructure must be obtained by simulation method.

2. Experimental

2.1. Preparation of simulated FGHAZ specimens

The material used was a P92 steel pipe with a 325 mm outer diameter and 40 mm wall thickness, which had been annealed and air cooled, followed by tempering at 1053 K for 6 h. The compositions of the steel were shown in Table 1. The average grain size of the steel was around 80 μm. The A_{c1} and A_{c3} temperatures of the P92 steel were 1093 and 1193 K, respectively. The FGHAZ was produced by Gleebe 2000 welding thermal simulator, inducing the heat cycles to the HAZ specimens. The specimens were heated rapidly to the peak temperature of about 1223 K and then cooled down to 473 K. PWHT was conducted at 1028 K for 5 h. The detailed thermal history for the preparation of simulated FGHAZ specimens was shown in Fig.1.

Table 1. Chemical compositions of the investigated P92 steel（wt%，bal. Fe）

C	Si	Mn	Cr	Mo	Ni	W	V	Nb	N	B	S	P
0.12	0.21	0.43	8.84	0.50	0.16	1.67	0.21	0.067	0.042	0.0033	0.004	0.014

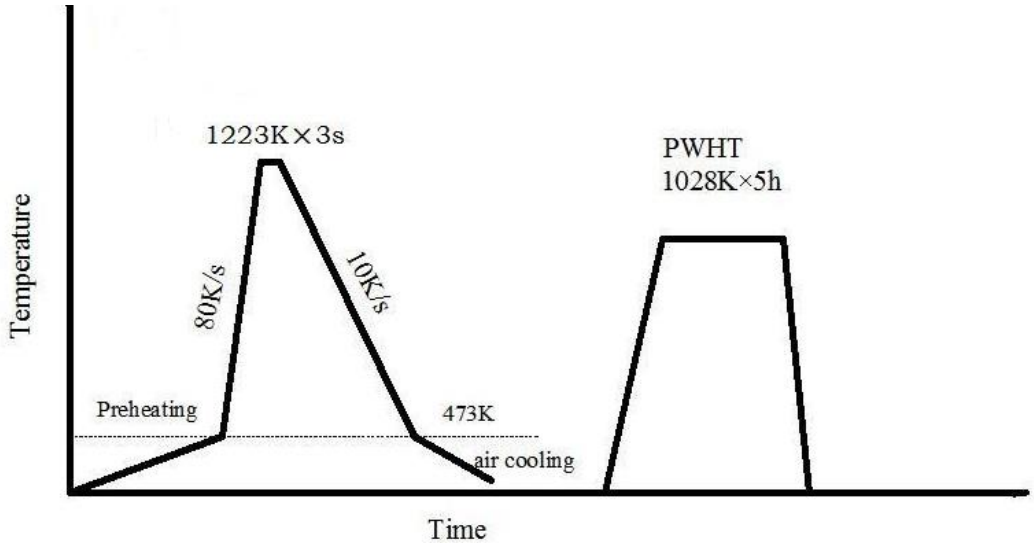

Fig.1. Preparation details of the specimens of FGHAZ reproduced by a weld simulator

2.2. Aging treatment

The simulated FGHAZ and base metal samples were both isothermally aged at 923 K for 100 h, 500 h, 1000 h, 1500 h, 2000 h, 3500 h, 4000 h and 5000 h. The hardness of the aged specimens was taken using a Brinell hardness tester with a force of 187.5 kgf. The microstructures of as-aged material were observed by optical microscopy. Specimens were prepared by mechanical polishing followed by etching in a solution of ethanol (100 ml), hydrochloric acid (5 ml) and picric acid (1 g) at room temperature.

2.3. SEM-BSE

Laves-phase with large mean atomic weight was distinguished from other precipitates in the materials using SEM-BSE method, and the BSE images were processed to binary images and measured with an image analysis system, similar to that reported by Dimmler et al. (2003). The statistical results of area fraction, number density and the mean equivalent circle diameter (ECD) of Laves-phase of the FGHAZ were obtained, thus its precipitation and coarsening kinetics can be deduced. These results were compared with those of base material.

2.4. TEM-EDS

A substructural investigation of thermally aged FGHAZ specimens was performed by conventional electron microscopy (TEM). Thin foils were prepared for observations of change in subgrain width and dislocation density. Carbon extraction replicas were prepared to avoid matrix effects during chemical analysis of the precipitates by energy dispersive X-ray spectroscope (EDS), and the crystal structure of precipitates was identified by electron beam diffraction pattern. At least ten particles of Laves-phase observed in the extraction replicas were measured by TEM-EDS for the typical aged condition specimens, and the mean value and the standard deviation of constituent elements can be obtained.

3. Results

3.1. Structural investigations

Fig.2 showed the optical micrographs of specimens for FGHAZ and BM with tempering and after aging at 923

K for 5000 h. Before thermal aging FGHAZ had a very fine prior austenite grain size of below 10 μm and hence the presence of the lath microstructure could not be identified. However, the base metal has a fairly larger grain size (around 80 μm) showing the typical lath martensite. This difference in mircostructures between the FGHAZ and BM still remained after aging at 923 K for 5000 h.

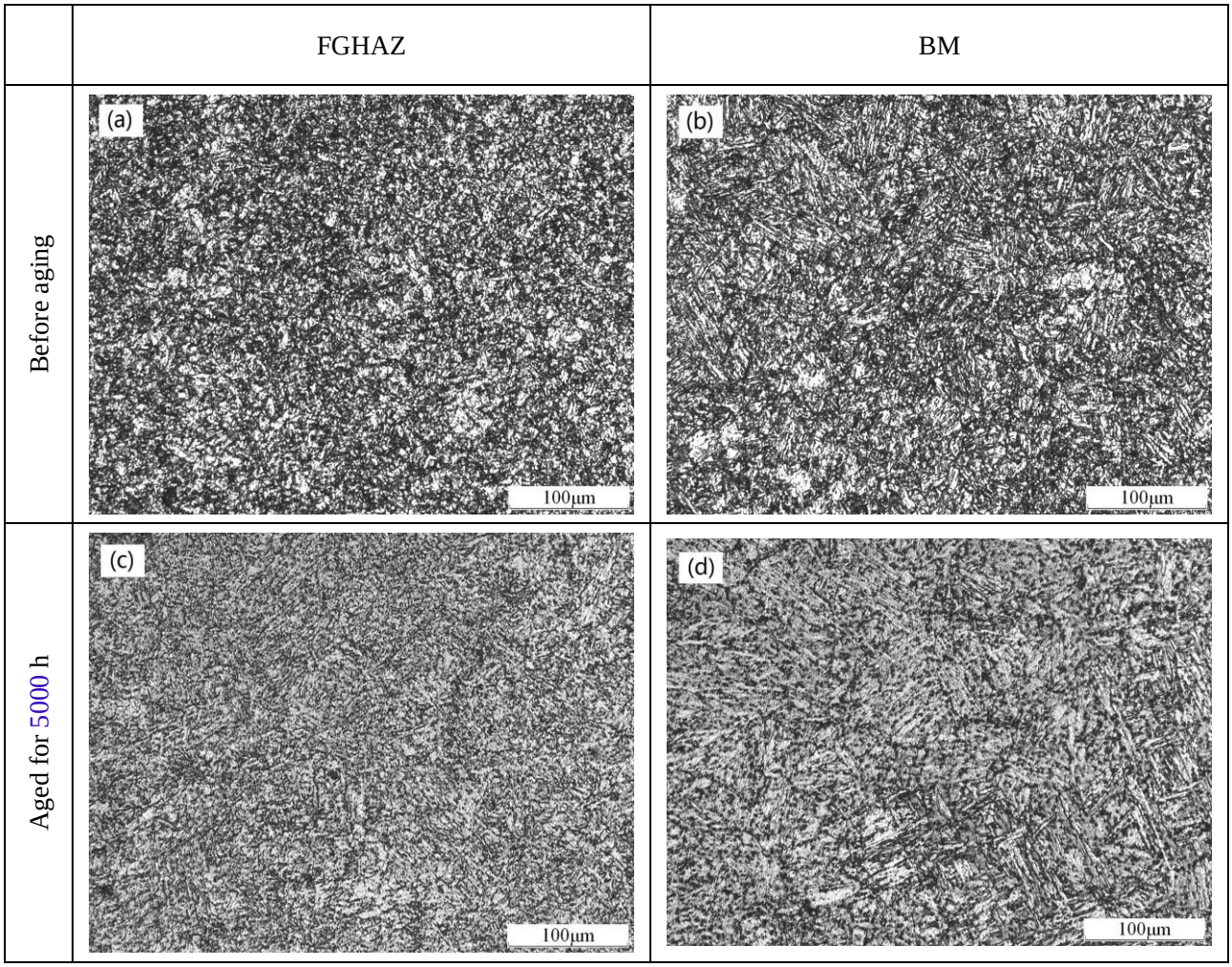

Fig.2. Optical micrographs of FGHAZ and BM before aging and after aging at 923 K for 5000 h

3.2. Quantification results of the Laves-phase

Fig.3 showed SEM-BSE images of specimens for FGHAZ and BM after aging at 923 K for 500 h, 2000 h and 5000 h, where the bright precipitates were identified as Laves-phase and the grey particles were identified as $M_{23}C_6$ carbides. MX carbonitrides were too small to be detected in SEM images. Laves-phase particles were observed on grain boundaries and laths boundaries in BM, however, they seemed to locate mostly on the grain boundaries in

FGHAZ. For specimens aged for the first 500 h, the Laves-phase precipitates in FGHAZ were found to be denser and smaller, indicating the much rapider precipitation of Laves-phase in FGHAZ. For specimens aged for 2000 h, the number density of Laves-phase in FGHAZ decreased slightly and its size increased. For specimens aged for 5000 h, the number density of Laves-phase dropped more drastically in FGHAZ (from 280 to 70 $10^3/mm^2$ for FGHAZ, 240 to 120 $10^3/mm^2$ for BM, refer to Fig.5b) and its size increase more markedly in FGHAZ (520 nm for FGHAZ and 400 for BM, refer to Fig.5c), revealed the faster coarsening of Laves-phase in FGHAZ. It was noted also that the coarsening of $M_{23}C_6$ carbides was not pronounced in both BM and FGHAZ during aging.

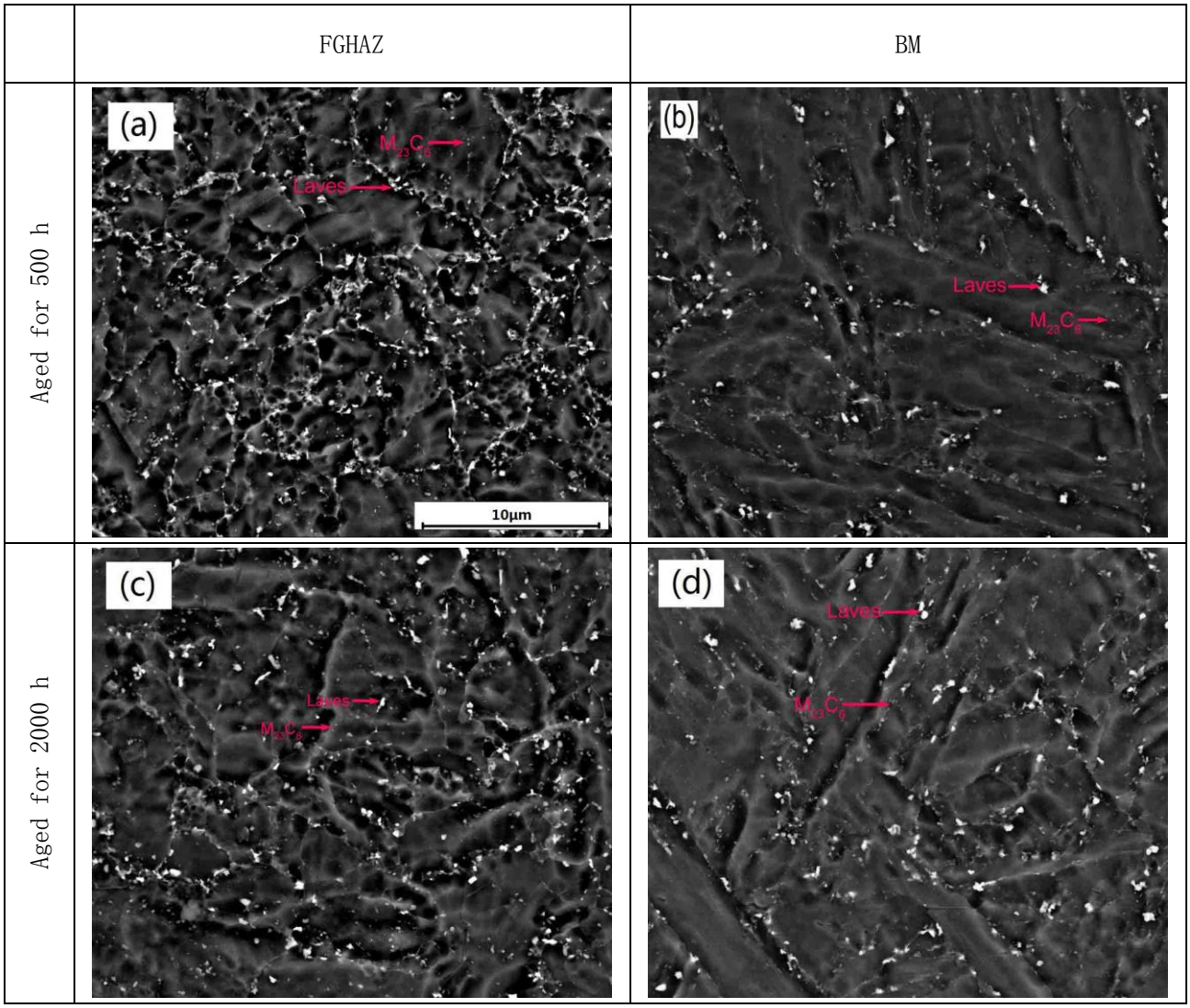

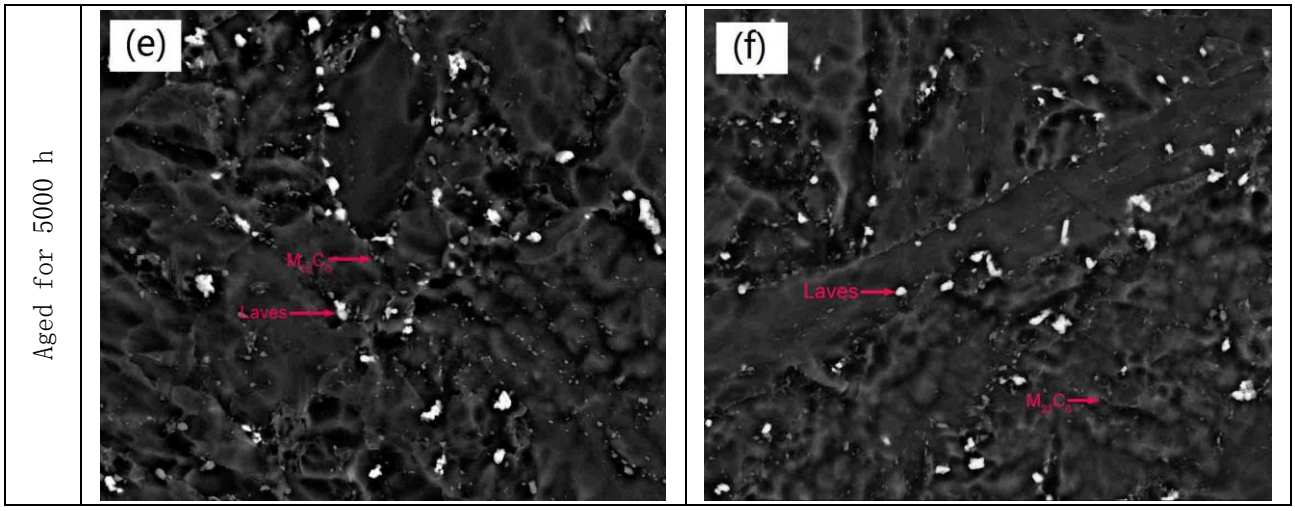

Fig.3. SEM-BSE micrographs of FGHAZ and BM aged at 923 K for 500 h, 2000 h and 5000 h

The distributions of equivalent circular diameters of the Laves-phase precipitates in FGHAZ and BM specimens aged for 500 h and 5000 h were shown in Fig.4. A normal distribution was adapted to the histogram resulting from the classification. The mode of the depicted normal distributions of Laves-phase in FGHAZ specimen aged for 500 h was smaller than that in BM. After ageing for 5000 h, the Laves-phase in FGHAZ shifted to a larger mean particle diameters (0.5 μm against 0.39 μm, Fig.4b), further indicating a rapider coarsening.

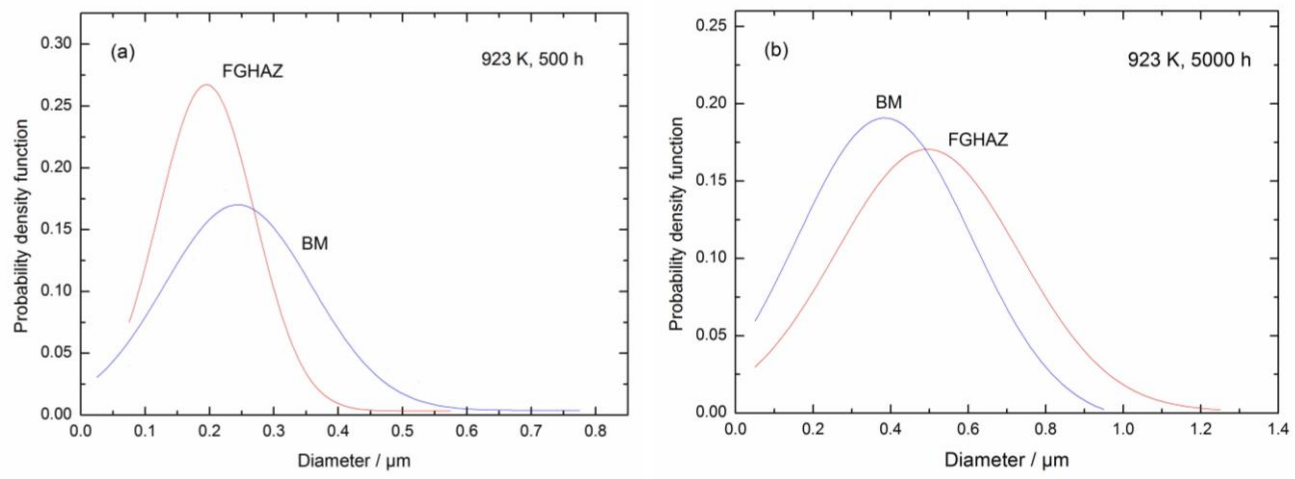

Fig.4.Comparison of the size distribution of Laves-phases in the FGHAZ and BM: after aged at 923 K for a) 500 h and b) 5000 h

The evolution of area fraction (equal to volume fraction), number density and corrected mean ECD of Laves-phase precipitates with time, were shown in Fig.5a-c. From Fig.5a-c, it can be seen about precipitation that 1) the area fraction and number density of Laves-phase precipitates in FGHAZ increased more quickly than that in BM with increasing time up to 1000 h; 2) the saturated value of the area fraction of around 1.0% was observed in

FGHAZ at 1000 hours, marking the completion of precipitation in FGHAZ; 3) the similar saturated value of area fraction was observed in BM, however, at about 1500 hours, which is 50% later. All these observations revealed that Laves-phase precipitates faster in FGHAZ than that in BM. From these Figures, it can also be seen about coarsening that 1) in the range of aging from 1000 h to 2000 h, the number density decreased and the equivalent diameter increased slowly in FGHAZ; 2)after 2000 h, the number density dropped abruptly and the equivalent diameter increased markedly in FGHAZ, indicating Ostwald ripening of precipitates; 3)the beginning of Laves-phase coarsening was earlier in FGHAZ than that in BM (as arrowed about 3000 h); and 4)after 3000 h, mean diameter of Laves-phase in the FGHAZ and BM increased to 520 nm and 400 nm, respectively, as shown in Fig.5c, revealing a faster coarsening of Laves-phase in FGHAZ.

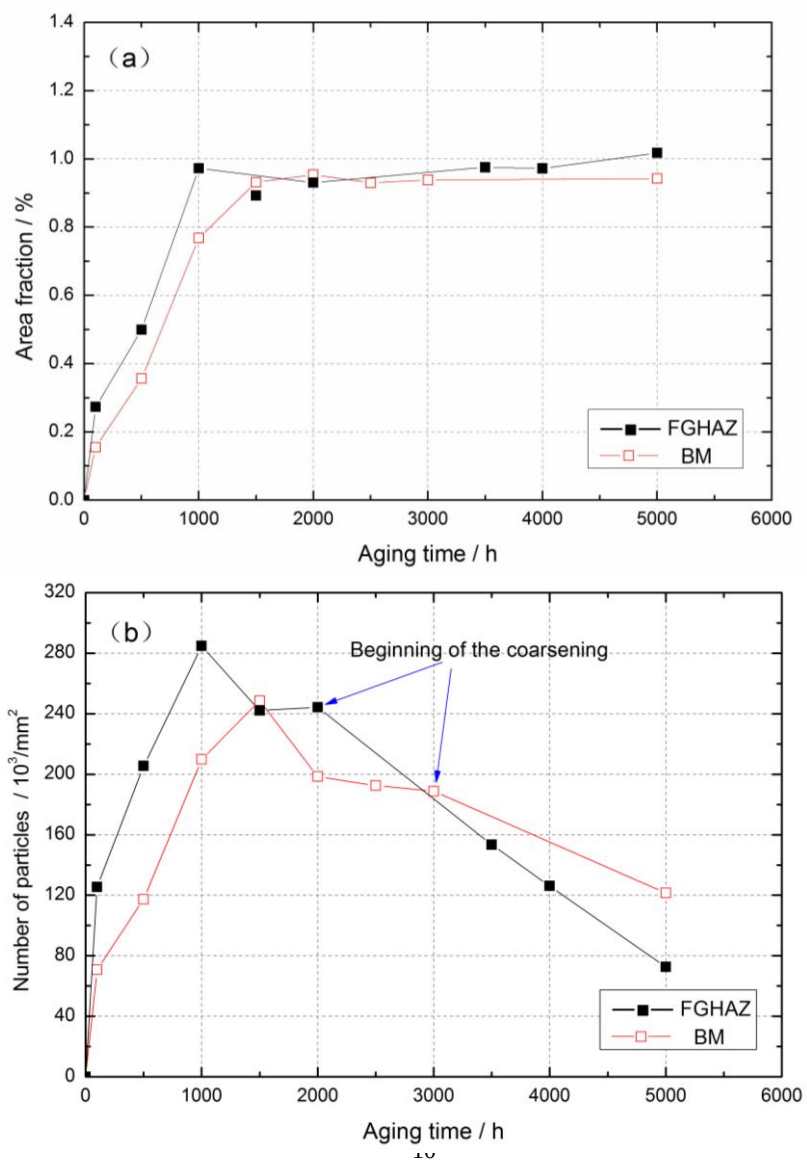

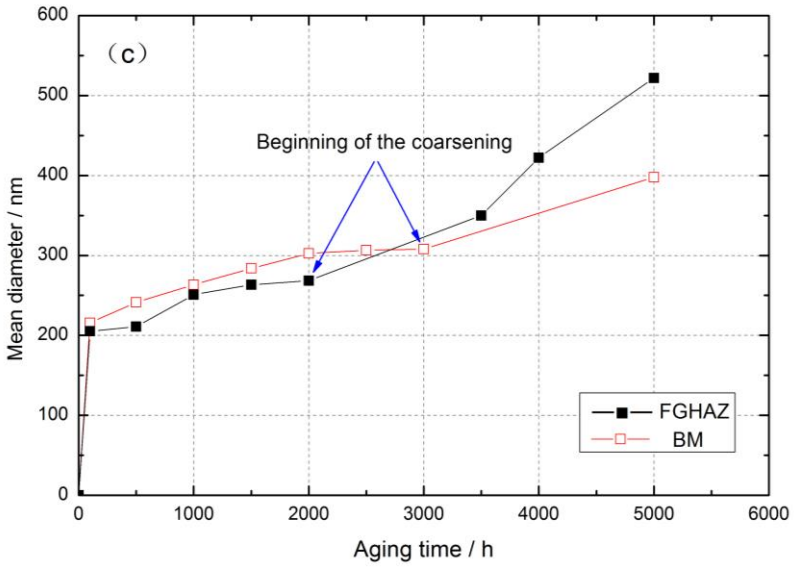

Fig.5. Quantification of Laves-phase precipitates in FGHAZ and BM aged at 923 K for up to 5000 h: （a）area fraction; （b）number of particles and（c）corrected mean ECD

3.3. Results of TEM-EDS

Fig.6 showed the TEM micrographs of the thin foil specimens for FGHAZ and BM with tempering and after aging at 923 K for 5000 h. The clear differences in initial microstructure between the FGHAZ and BM can be observed from Fig.6a and b. The FGHAZ exhibited the coarse polygonal subgrains with low dislocation density in interiors replacing the lath martensite structure of BM, and the change in morphology of $M_{23}C_6$ carbides on subgrain boundaries can also be found from plate-like to spherical shape. The MX carbonitrides of FGHAZ were unchanged compared to BM, mainly distributed within the subgrains and were fine and stable. The microstructural changes in the FGHAZ were ascribed to the instability of lath martensitic microstructure formed by welding thermal cycle, contributing to the partial annihilation of the martensite lath structure and the recovery of dislocation within subgrains in subsequent PWHT, resulting in the formation of coarse polygonal subgrains. Fig.6d showed that the remains of tempered lath substructure could still be distinguished in BM subjected to aging at 923 K for 5000 h, which have confirmed by the optical microscopy as shown in Fig. 2d. Fig.6c and d also revealed the increase in subgrain width in aged FGHAZ and BM respectively.

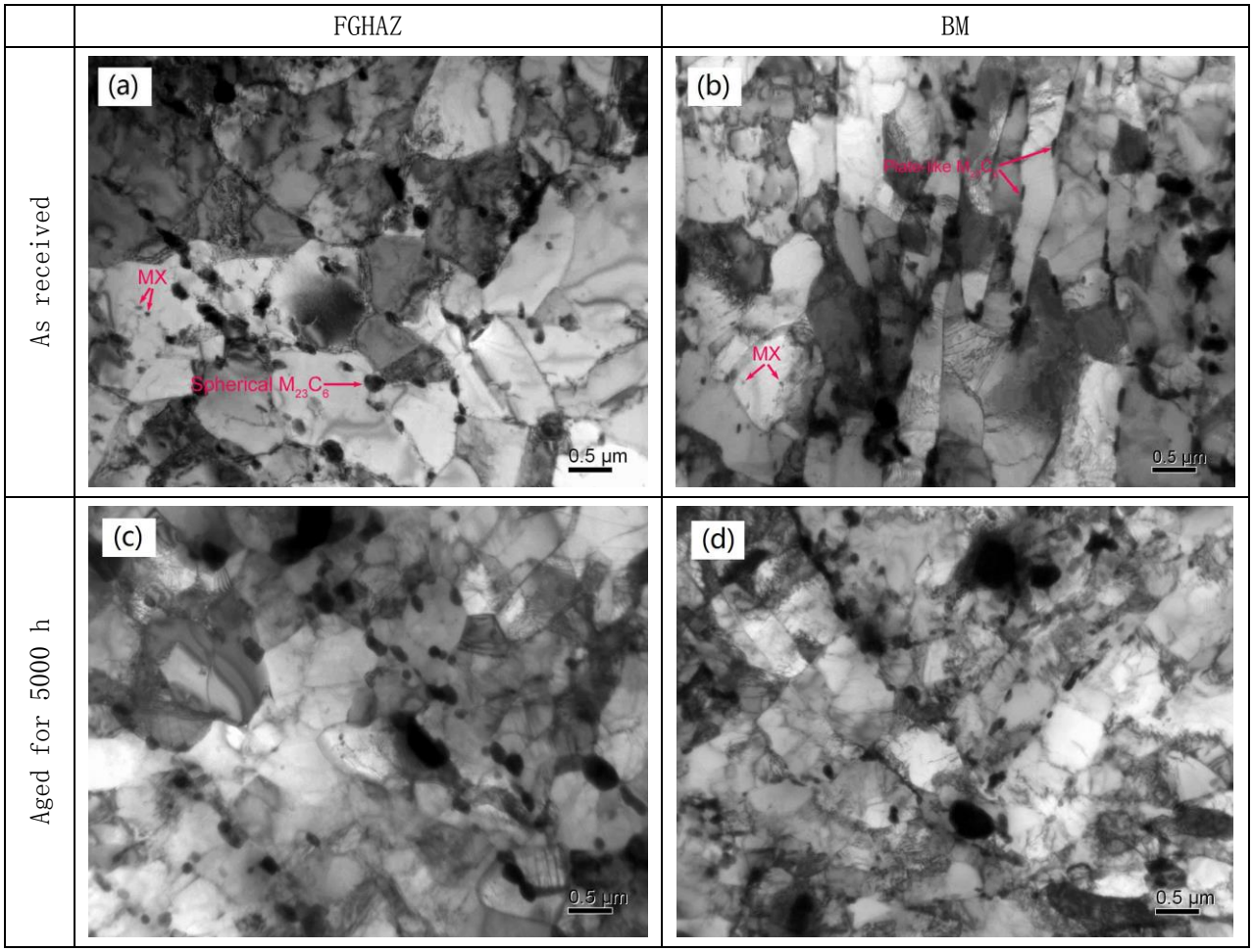

Fig.6. TEM thin micrographs of FGHAZ and BM as received (a) and (b) and aged at 923 K for 5000 h (c) and (d)

Carbon extraction replicas of the FGHAZ and BM specimens after aging for 500 h and 5000 h were shown in Fig. 7. EDS microanalysis confirmed that the minor precipitates were MX, the less fine and the large precipitates were $M_{23}C_6$ and Laves-phase, respectively. It was found that the FGHAZ had the higher number density and smaller size of Laves-phase than BM at aging for the first 500 h (Fig. 7a and b). After aging for 5000 h, FGHAZ exhibited the faster coarsening of Laves-phase with the larger size than BM (Fig. 7c and d). The observations by TEM were in agreement with those by SEM, revealing that the rapider precipitation and coarsening of Laves-phase in FGHAZ than in BM.

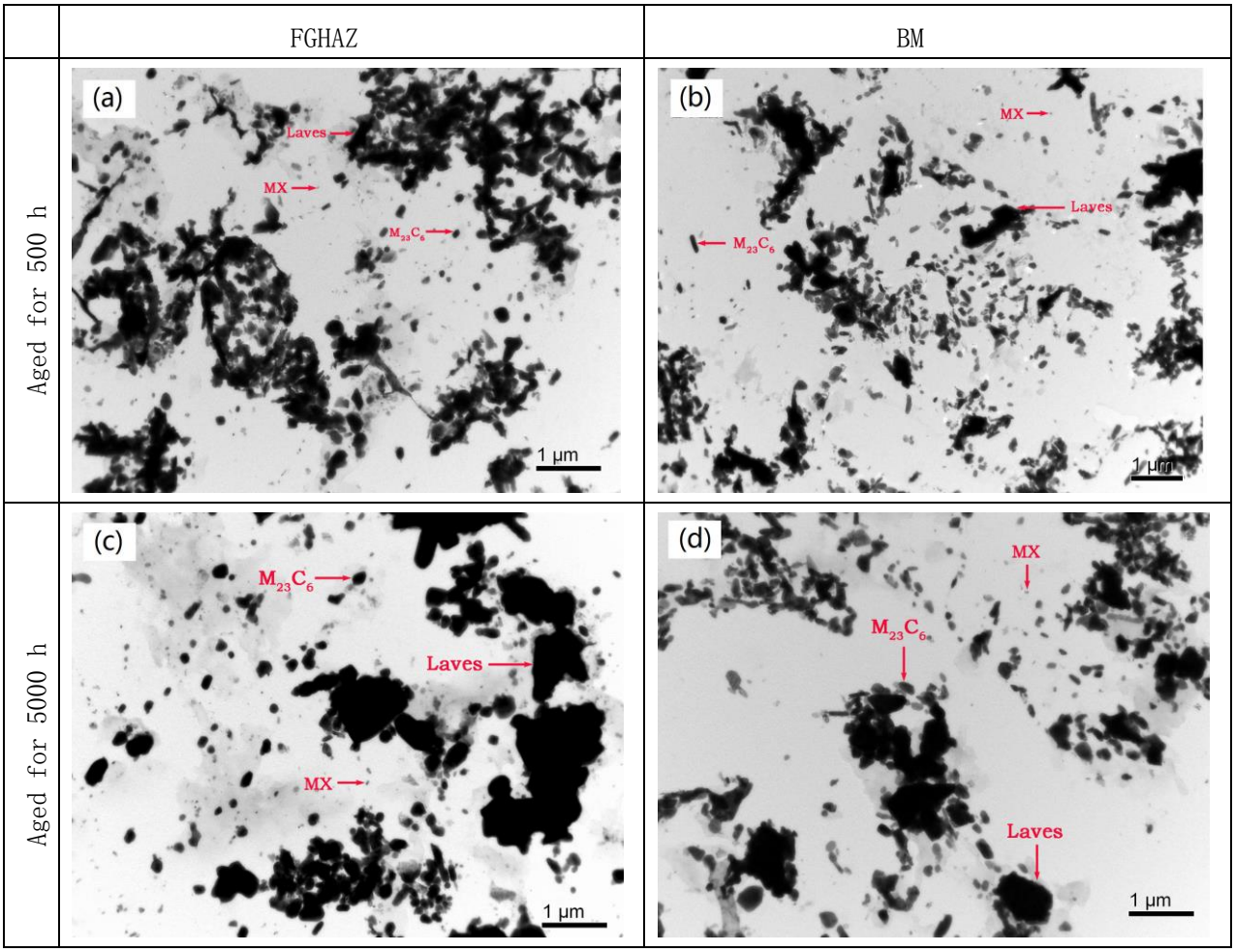

Fig.7. TEM micrographs of the replicas of FGHAZ and BM aged at 923 K for 500 h (a) and (b) and for 5000 h（c）and (d)

Fig.8 showed the identification of irregular coarse precipitate by diffraction analysis with extraction replica from FGHAZ specimen aged at 923 K for 2000 h, further confirmed that the coarse precipitates were Laves-phase with primitive hexagonal lattice. The average chemical composition of Laves-phase measured by EDS in FGHAZ under different aging conditions was given in Table 2, indicated that this phase was rich in Cr and Mo in addition to Fe and W. The compositions of Laves-phase in FGHAZ remained similar except Cr (from 15% to 10%) during aging.

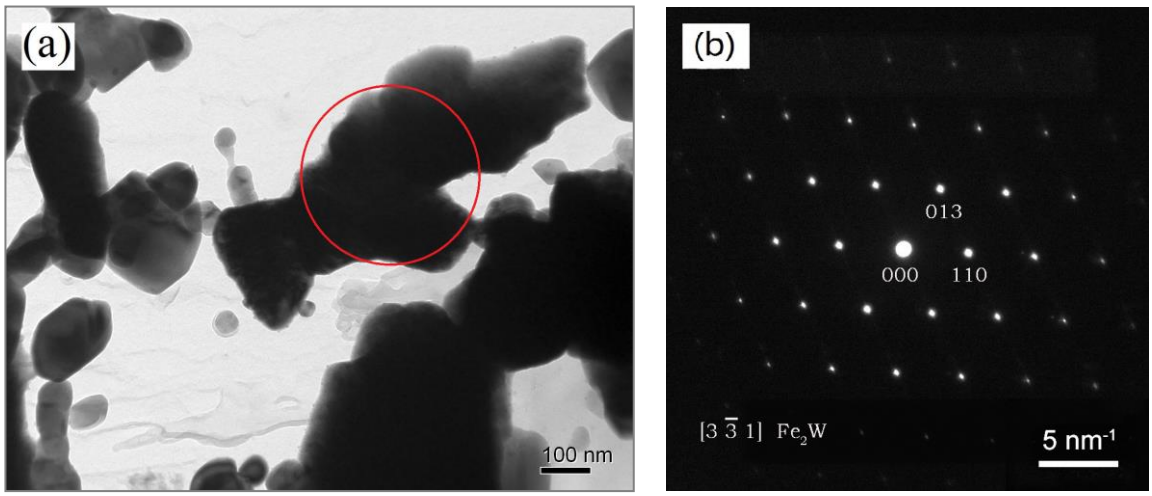

Fig.8. Identification of coarse precipitates by diffraction analysis with extraction replica from FGHAZ specimen aged at 923 K for 2000 h, (a)bright field image,（b）selected area diffraction pattern

Table 2. Results from EDS analyses of Laves-phase of FGHAZ (in normalised at.%)

Aging conditions	Cr	Fe	Mo	W
923 K, 500 h	15.09±1.22	47.77±0.92	10.42±0.76	26.72±1.26
923 K, 2000 h	16.34±4.02	48.17±1.73	8.41±0.51	27.08±1.93
923 K, 5000 h	10.60±0.50	51.31±0.86	8.67±0.67	29.43±0.88

3.4. Hardness measurement

Fig.9 showed the change of hardness as a function of aging time. The hardness of the tempered FGHAZ specimen was lower than that of BM (about 230 HB) before aging. The softening of FGHAZ was due to the recovery and polygonization of the lath martensite during PWHT, as described above. In the early stage of aging, the change in the hardness of FGHAZ was little with increasing time, indicated precipitation hardening through the fine Laves-phase precipitates just made up for a loss of solid solution hardening produced by the droplet of solute atom W and Mo in matrix. After aging for 2000 h, the pronounced loss of hardness can be found in FGHAZ, and this may be closely correlated to the coarsening of Laves-phase precipitates.

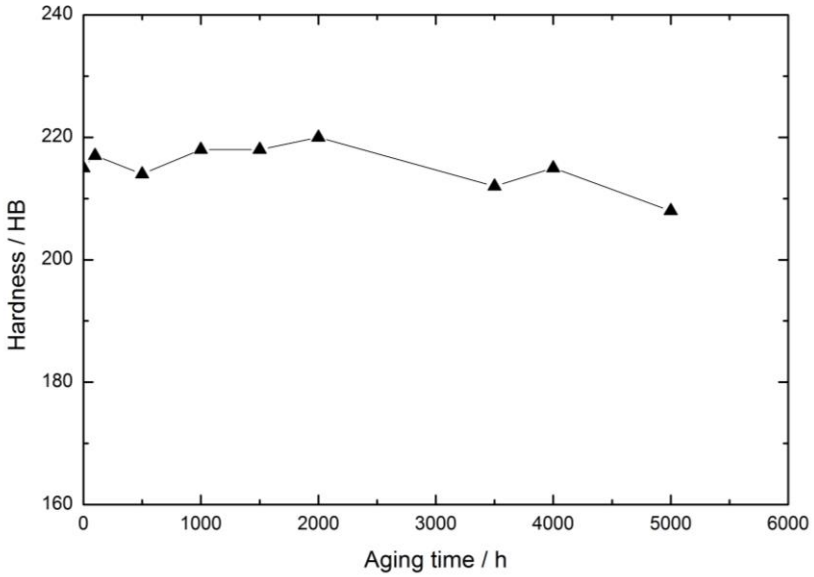

Fig.9. Change of hardness in the FGHAZ as a function of aging time at 923 K

4. Discussion

4.1. Kinetics of Laves-phase precipitation in FGHAZ

The precipitation of Laves-phase completes at aging for around 1000 h as described previously. The time-dependent volume fraction *f* of a secondary phase can be described using the Johnson-Mehl-Avrami equation:

$$f(t) = 1 - e^{-(\frac{t}{t_0})^n} \qquad (1)$$

where t_0 is a time constant and n is a time exponent.

The discrete experimental data of the volume fraction and time for FGHAZ was plotted in Fig.10. The value of the time exponent n is the gradient of these points. Linear regression up to 1000 h found n is about 0.52. Long (2006) indicated that the time exponent is 1/2 in the case of secondary phase precipitates nucleation at grain boundaries or phase boundaries and the nucleation rate rapidly decreases to zero. Therefore, Laves-phase in FGHAZ should precipitate on the grain boundaries according to the time exponent n close to 1/2, which was confirmed with a distribution of Laves-phase in SEM images as shown in Fig.3. The fine prior austenite grains in the FGHAZ resulted in higher boundary area of prior austenite per unit volume compared to BM, provided more preferred nucleation sites for Laves-phase, thus accelerated its precipitation.

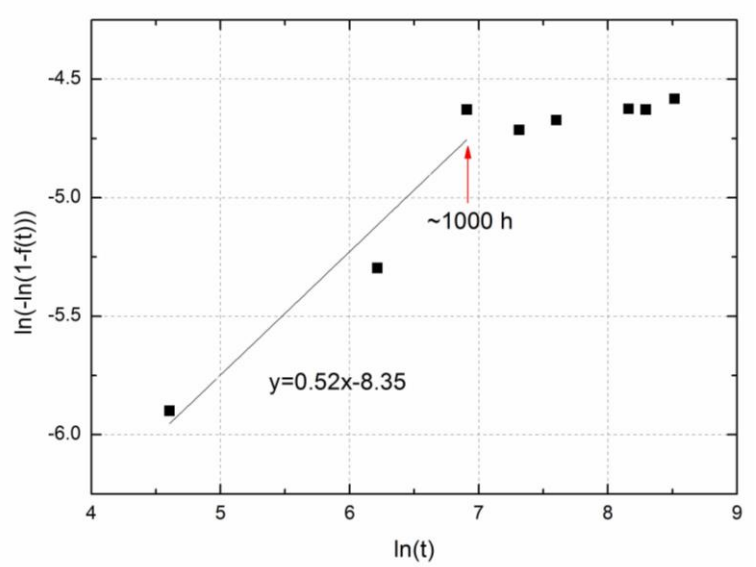

Fig.10. Evaluation of time exponent *n* based on the quantification results of Laves-phase precipitates in FGHAZ at 923 K

4.2. Coarsening of Laves-phase

The coarsening of Laves-phase precipitates in FGHAZ was described by the following Ostwald ripening equation:

$$r^m - r_0^m = K_p t \qquad (2)$$

where r_0 and r is the average radius of particles at the beginning of coarsening and at a given time t, and K_p is a constant. The exponent m is 3 for the coarsening controlled by volume diffusion. In a multi-phases system of β precipitate in a matrix, the coarsening rate constant K_p can be calculated theoretically the following formula given by Ågren et al.(2000) :

$$K_p = \frac{8}{9} \frac{\gamma V_m^{\beta}}{\sum_{i=1}^{c} \frac{(x_i^{\beta} - x_i^{\alpha/\beta})^2}{x_i^{\alpha/\beta} D_i / RT}} \qquad (3)$$

As above γ is the interfacial energy and V_m^{β} is the molar volume of the precipitate phase. D_i is the diffusion coefficient of element i in the matrix, X_i^{β} is the molar fraction of element i in the precipitate and $X_i^{\alpha/\beta}$ is the molar fraction of element i at the precipitate /matrix interface (often used as X_i^{α}, the molar fraction of element i in the matrix). R is the gas constant and T is the temperature. The value of γ for is 1 Jm^{-2} due to incoherent coarse Laves-phase particle/matrix interfaces. V_m^{β} =4.57×10^{-8} m^3 for Laves phase, D_W=2.22×10^{-17} m^2/s and D_{Mo}=9.6×10^{-17}

m^2/s for α-Fe at 923 K. The values of X_i^{β} and X_i^{α} were evaluated using Thermo-Calc and they are 29.18% and 0.27%. The calculated value of K_p was 3.80×10^{-30} m^3/s by equation Eq.(3) in the case of m=3 (coarsening controlled by volume diffusion).

Fig.11 showed the experimental value of K_p for FGHAZ was 1.38×10^{-27} m^3/s by equation Eq.(3) assuming coarsening controlled by volume diffusion (m=3). This is much greater than that of theoretical calculation, revealing that the volume diffusion was not the main cause of Ostwald ripening of Laves-phase precipitates in FGHAZ. Thus, grain boundary diffusion must play the dominant role in its coarsening. Similarly, the experimental value of K_p for BM was 3.72×10^{-28} m^3/s, it also revealed that the coarsening of Laves-phase precipitates in BM is also not volume diffusion controlled, and it is of grain boundary diffusion. The relative smaller K_p value for BM is shown by Fig.11. Fast coarsening of Laves-phase precipitates observed in FGHAZ rather than in BM was attributed to the increase in grain boundary diffusion which, in turn, was resulted from the finer prior austenite grains in FGHAZ.

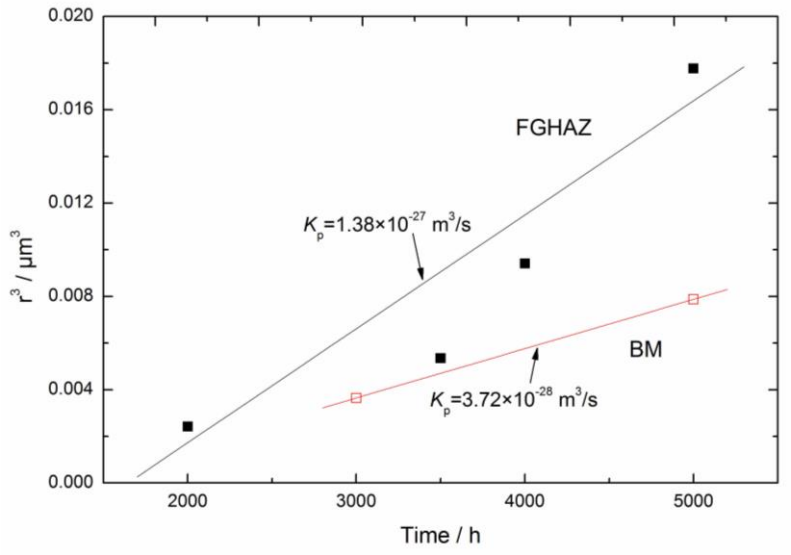

Fig.11. Comparison of the coarsening curves of Laves-phase precipitates between FGHAZ and BM at 923 K

4.3. Effect of Laves-phase precipitation on creep properties of FGHAZ and type Ⅳ fracture in welded joints

The precipitated Laves-phase may contribute to the creep rupture strength by dispersion hardening. In the early aging (before coarsening), in comparison with BM, FGHAZ had rapider precipitation of Laves-phase due to the fine prior austenite grain, resulting in a denser and smaller size of Laves-phase precipitates, therefore enhanced the creep rupture strength. However, the dispersion hardening contribution of Laves-phase precipitates in FGHAZ may drop abruptly due to its fast coarsening during the long-term aging. Hald (2000) has given the Orowan stress due to precipitates formula described by Eq. (4)

$$\sigma_{Orowan} = 3.32Gb\frac{\sqrt{f_p}}{d_p} \qquad (4)$$

where G is the shear modulus (64 GPa at 923 K, b is the length of Burgers vector (0.25 nm), f_p is the precipitate volume fraction and d_p is the mean precipitate diameter. Table 3 compared with Orowan stress of Laves-phase precipitates in FGHAZ and BM, obtained from Eq. (4). It showed that Orowan stress of Laves-phase precipitates in FGHAZ was 40 percent higher than that of BM at aging for the first 500 h, due to its fine size and high number density. However, the lower Orowan stress was found in FGHAZ at aging for 5000 h compared to BM, owing to the coarser Laves-phase precipitates. It can be concluded that the strengthening contribution of Laves-phase precipitates in FGHAZ was minor under low stress and long-term creep, consequently it can not retard the degradation of creep rupture strength of FGHAZ. The variation of precipitation strengthening of Laves-phase in FGHAZ can explain for the change of its hardness during aging as shown in Fig.9. In the early aging (before coarsening of Laves-phase precipitates), hardness in FGHAZ did not drop with increasing time due to its precipitation strengthening exactly compensating the loss of solid solution hardening, while after aging for 2000 h, loss of hardness in FGHAZ occurred due to the fast coarsening of Laves-phase precipitates.

Table 3. Comparison of Orowan stress of Laves-phase precipitates in FGHAZ and BM

Aging conditions	Volume fraction *f*p (%)		Diameter *d*p (nm)		Orowan stress σ_{or}（MPa）	
	BM	FGHAZ	BM	FGHAZ	BM	FGHAZ
923 K, 500 h	0.36	0.50	241	210	13	18
923 K, 2000 h	0.95	0.93	303	269	17	19
923 K, 5000 h	0.94	1.01	398	522	13	10

Lee et al.（2006）have reported that coarse Laves-phase on grain boundaries acted as the preferential site of cavity, resulting in intergranular brittle fracture and abrupt reduction of the creep strength of the P92 steel during long-term creep. Shinozaki et al. (2002) and Wang et al. (2012) discovered that Type Ⅳ fracture also exhibited brittle intergranular fracture produced by the growth and coalescence of cavities in the FGHAZ of a welded joint, and coarse Laves-phase precipitates acted as sites for the nucleation. It is generally believed that cavities are nucleated due to grain boundary sliding at geometrical irregularities (inclusion or secondary-phase particles) on grain boundaries, where high local stress concentrations could develop. Sklenička (1996) indicated that the association of cavities with secondary-phase particles on grain boundaries in creep-resistant steels had been frequently observed. The greater size of precipitate on grain boundaries was, the more serious concentration of stress-strain was and more easily contributed to the initiation of creep cavities. The coarsening of Laves-phase precipitates was faster in FGHAZ than BM, as a result a stronger tendency for creep void to occur in FGHAZ during long-term creep. Secondly, Dejun and Shinozaki (2005) investigated the effect of material properties of the matrix on the stress-strain distributions of the interface between the precipitate and matrix, and the results showed that the equivalent strain rate at the FGHAZ matrix / precipitate interface can be enhanced by the softer matrix of recovered coarse polygonal subgrains with low dislocation density comparing with the base metal as described above, leading to more creep void initiation. Lastly, Albert et al. (2005) suggested that the multiaxial stress state in the FGHAZ introduced by obvious creep properties heterogeneity of the different zone in a welded joint, facilitated

the growth of these cavities into large cavities which coalesce to form microcracks and subsequently lead to final fracture. From the above discussion, it can be concluded that the difference in evolution behavior of Laves-phase precipitates during long-term exposure between FGHAZ and BM was one of a major factor for Type Ⅳ fracture of a welded joint, other than the changes in initial microstructures, e.g no lath martensite structure, coarsening of $M_{23}C_6$ carbides and so on, taken place in weld thermal cycle and subsequent post weld heat treatment.

Abe et al.(2007) have found that the 9Cr steels with increase in boron content combined with minimized nitrogen as low as 10-20 ppm suppressed grain refinement in the HAZ of welded joints and hence suppressed Type Ⅳ cracking in welded joints. He proposed that not only boundaries but also subboundaries were covered by $M_{23}C_6$ carbides after A_{c3} heat cycle, which were substantially the same as those in the base metal, their hardening were the most important factor. The contribution of delaying Laves-phase evolution produced by no fine grain formed in HAZ are probably responsible for avoiding the degradation of creep strength in HAZ during long-time creep.

5. Conclusions

The precipitation and coarsening of Laves-phase in simulated fine grained heat-affected zone（FGHAZ）for P92 steel during aging at 923 K were investigated and compared to base metal (BM). The results are summarized as follows.

- Laves-phase precipitates mostly on grain boundaries in FGHAZ.
- Due to faster precipitation, saturation of the area fraction of Laves-phases was observed in the FGHAZ rather than in BM.
- The coarsening rate of Laves-phase precipitates in FGHAZ was greater than that in BM.
- In comparison with BM, the FGHAZ had denser and smaller Laves-phase precipitates during the early aging, enhanced the creep strength by precipitation hardening, however, this effect in FGHAZ reduced abruptly due to the more profound coarsening on the completion of its precipitation.

- The grain refinement in FGHAZ changed the evolution behavior of the Laves-phase precipitates, contributing in the formation of the cavities during long-term creep. This indirect effect may play significant role in Type Ⅳ fracture of a welded joint in 9% Cr steels except for the degradation of the initial microstructure occurred in welding and the following post -weld heat treatment（PWHT）.

References

Abe F., Tabuchi M., 2004. Microstructure and creep strength of welds in advanced ferritic power plant steels. Sci. Technol. Weld. Joining. 9, 22-30.

Abe F., Tabuchi M., Kondo M., Tsukamoto S., 2007. Suppression of Type Ⅳ fracture and improvement of creep strength of 9Cr steel welded joints by boron addition. J. Pres. Ves. Technol. 84, 44-52.

Ågren J., Clavaguera-Mora M T, Golcheski J., Inden G., Kumar H., Sigli C., 2000. Calphad. 24, 41-54.

Albert S K., Tabuchi M., Hongo H., Watanabe T., Kubo K., Matsui M., 2005. Effect of welding process and groove angle on type Ⅳcracking behaviour joints of a ferritic steel. Sci. Technol. Weld. Joining. 10, 149-157.

Dejun L., Shinozaki K., Kuroki H., Harada H., Ohishi K., 2003. Analysis of factors affecting type Ⅳcracking in welded joints of high chromium ferritic heat resistant steels. Sci. Technol. Weld. Joining. 8, 296-302.

Dejun L., Shinozaki K., 2005. Simulation of role of precipitate in creep void occurrence in heat affected zone of high Cr ferritic heat resistant steels. Sci. Technol. Weld. Joining. 10, 544-549.

Dimmler G., Weinert P., Kozeschnik E., Cerjak H., 2003. Quantification of the Laves phase in advanced 9-12% Cr sreels using a standard SEM. Mater. Charact. 51, 341-52.

El-Azim M.E.A., Nasreldin A.M., Zies G., Klenk A., 2005. Microstructural instability of a welded joint in P91steel during creep at 600℃. Mater. Sci. Technol. 21, 779-790.

Hald J., 2008. Microstructure and long-term creep properties of 9-12%Cr steels. J.Pres Ves Technol. 85, 30-37.

J. Parker, 2013. In-service behavior of creep strength enhanced ferritic steels Grade 91 and Grade 92- Part 1 parent metal. J. Pres. Ves. Technol. 101, 30-36.

Lee J S, Armaki H G, Maruyama K., Muraki T., Asahi H., 2006. Causes of breakdown of creep strength in 9Cr-1.8W-0.5Mo-VNb steel. Mater. Sci. Eng. A . 428, 270-275.

Letofsky E, Cerjak H, 2004. Metallography of 9Cr steel power plant microstructures. Sci. Technol. Weld. Joining. 8, 296-302.

Long Y Q., Secondary phase in steels (China). Metallurgical Industry Press，Beijing, 2006.

Matsui M., Tabuchi M., Watanabe T., Kubo K., Kinugawa J., Abe F., 2001. Degradation of creep strength in welded joint of 9%Cr steel. ISIJ International. 41s, 126-130.

Muramatasa K., in :Viswanathan R, Nutting J (Eds),1998. Proceedings of the Advanced Heat Resistant Steels for Power Generation, The University Press, Cambridge, P. 543.

Shinozaki K.,Dejun L., Kuroki H., Harada H., Ohishi K., 2002. Analysis of degradation of creep strength in heat-affected zone of weldment of high Cr heat-resisting steels basedd on void observation. ISIJ International. 42, 1578-1584.

Sklenička V, In: Moura-Branco C, Ritchie R, Sklenička V, editors. 1996. Mechanical behaviour of materials at high temperature. Dordrecht (the Netherlands): Kluwer Acadamic Publishing, 43-58.

Tshuchida Y., Okamoto K., Tokunaga Y., 1995. Improvement of creep rupture strength of 9Cr-1Mo-V-Nb-N steel by thermo-mechanical control process. ISIJ International. 35, 317-323.

Tsuchida Y, Okamato K, Tokunaga Y, 1996. Study of creep rupture strength in heat affected zone of 9Cr-1Mo-V-Nb-N steel by welding thermal cycle. Welding Joining International. 10, 27-33.

Wang X., Pan Q G., Ren Y Y., Shang W., Zeng H Q., Liu H., 2012. Microstructure and Type Ⅳ cracking behaviour of HAZ in P92 steel weldment. Mater. Sci. Eng. A. 552, 493-501.

Wang X., Xu Q., Liu H W., Liu H., Shang W., Ren Y Y., Yu S M., 2014. On the method for reproducing fine grained HAZ of W strengthened high Cr steel. Mater. Sci. Eng. A. 589, 50-56.

Xu Q., Lu Z., Wang X., Damage Modelling: the current state and the latest progress on the development of creep damage constitutive equations for high Cr steels, in HIDA-6 Conference: Life/DefectAssessment&Failures in High Temperature Plant, 2nd - 4th December 2013, Nagasaki, Japan

Acknowledgements

The author would like to express their gratitude for projects supported by the National Natural Science Foundation of China (51074113 and 51374153) and Sichuan Province Fundamental Research Project （2013JY0123）.

Tables and figure legends

Table 1. Chemical compositions of the investigated P92 steel（wt%，bal. Fe）

C	Si	Mn	Cr	Mo	Ni	W	V	Nb	N	B	S	P
0.12	0.21	0.43	8.84	0.50	0.16	1.67	0.21	0.067	0.042	0.0033	0.004	0.014

Table 2. Results from EDS analyses of Laves-phase of FGHAZ (in normalised at.%)

Aging conditions	Cr	Fe	Mo	W
923 K, 500 h	15.09±1.22	47.77±0.92	10.42±0.76	26.72±1.26
923 K, 2000 h	16.34±4.02	48.17±1.73	8.41±0.51	27.08±1.93
923 K, 5000 h	10.60±0.50	51.31±0.86	8.67±0.67	29.43±0.88

Table 3. Comparison of Orowan stress of Laves-phase precipitates in FGHAZ and in BM

Aging conditions	Volume fraction *f*p (%)		Diameter *d*p (nm)		Orowan stress σ_{or}（MPa）	
	BM	FGHAZ	BM	FGHAZ	BM	FGHAZ
923 K, 500 h	0.36	0.50	241	210	13	18
923 K, 2000 h	0.95	0.93	303	269	17	19
923 K, 5000 h	0.94	1.01	398	522	13	10

Fig.1. Preparation details of the specimens of FGHAZ reproduced by a weld simulator

Fig.2. Optical micrographs of FGHAZ and BM before aging and after aging at 923 K for 5000 h

Fig.3. SEM-BSE micrographs of FGHAZ and BM aged at 923 K for 500 h, 2000 h and 5000 h

Fig.4. Comparison of the size distribution of Laves-phases in the FGHAZ and BM: after aged at 923 K for a) 500 h and b) 5000 h

Fig.5. Quantification of Laves-phase precipitates in FGHAZ and BM aged at 923 K for up to 5000 h: （a）area fraction; （b）number of particles and（c）corrected mean ECD

Fig.6. TEM thin micrographs of FGHAZ and BM as received (a) and (b) and aged at 923 K for 5000 h (c) and

(d)

Fig.7. TEM micrographs of the replicas of FGHAZ and BM aged at 923 K for 500 h (a) and (b) and for 5000 h（c）and (d)

Fig.8. Identification of coarse precipitates by diffraction analysis with extraction replica from FGHAZ specimen aged at 923 K for 2000 h, (a)bright field image,（b）selected area diffraction pattern

Fig.9. Change of hardness in the FGHAZ as a function of aging time at 923 K

Fig.10. Evaluation of time exponent *n* based on the quantification results of the area fraction of Laves-phase precipitates in FGHAZ at 923 K

Fig.11. Comparison of the coarsening curves of Laves-phase precipitates between FGHAZ and BM at 923 K